

**THE IN-FLIGHT CALIBRATION
OF THE HUBBLE SPACE TELESCOPE FINE GUIDANCE SENSORS - II
(A SUCCESS STORY)**

G. Welter
Computer Sciences Corporation

L. Abramowicz-Reed
Hughes Danbury Optical Systems

A. Guha
AKG Incorporated

L. Hallock
National Aeronautics and Space Administration / Goddard Space Flight Center

and E. Kimmer
AlliedSignal Technical Services Corporation

ABSTRACT

The Hubble Space Telescope's fine guidance sensors (FGSs) are unique in the performance levels being attempted; spacecraft control and astrometric research with accuracies better than 3 milliarcseconds (mas) are the ultimate goals. This paper presents a review of the in-flight calibration of the sensors, describing both the algorithms used and the results achieved to date. The work was done primarily in support of engineering operations related to spacecraft pointing and control and secondarily in support of the astrometric science calibration effort led by the Space Telescope Astrometry Team. Calibration items of principal interest are distortion, sensor magnification, and relative alignment. An initial in-flight calibration of the FGSs was performed in December 1990; this calibration has been used operationally over the past few years. Followup work demonstrated that significant, unexpected temporal variations in the calibration parameters are occurring; provided good characterization of the variations; and set the stage for a distortion calibration designed to achieve the full design accuracy for one of the FGSs. This full distortion calibration, using data acquired in January 1993, resulted in a solution having single-axis residuals with a standard deviation of 2.5 mas. Scale and alignment calibration results for all of the FGSs have been achieved commensurate with the best ground-based astrometric catalogs (root-mean-square error ~ 25 mas). A calibration monitoring program has been established to allow regular updates of the calibration parameters as needed.

1. INTRODUCTION AND BACKGROUND

The Hubble Space Telescope (HST) began its mission in April 1990. The ultimate scientific goals require relative pointing accuracy of order 3 milliarcseconds (mas) for target objects within the telescope's 0.5-degree-diameter field of view (FOV). This high accuracy is achieved using the spacecraft's fine guidance sensors (FGSs), manufactured by Hughes Danbury Optical Systems (HDOS), which allow the spacecraft to maintain pointing relative to a preselected set of guide stars. The milliarcsecond-level pointing requirements dictate equally demanding requirements for the FGS calibration algorithms and procedures. Refs. 1 and 2 presented a summary of the status of our calibration efforts as of mid-summer 1991, at which time calibration results had not yet achieved the design accuracy level. This paper presents the results of our continued calibration work through the time of the HST First Servicing Mission (FSM) at the end of 1993.

Besides a calibration error level an order of magnitude above the design level, Refs. 1 and 2 also reported initial indications of unexpected temporal variations in the FGS calibration parameters. The variations, based on a comparison of data taken in December 1990 and May 1991, were noted in both optical field angle distortion (OFAD) of the individual FGSs and the relative alignments of the FGS FOVs. The OFAD changes were detected at essentially the 1σ noise level (~ 30 mas) of the reference catalog used for the calibrations, whereas the alignment changes were about a factor of seven above the noise. Because of the low level of

certainty in the initial OFAD change detection, precise differential analysis of apparent motions of the same target stars from the preceding year was performed in December 1991. This analysis, being independent of the ground-based catalog, was able to verify the previously detected OFAD change rate at a level an order of magnitude above noise.

Section 5 discusses the results of our December 1991 and subsequent analyses of FGS calibration variation. At the time of our verification of the sensor changes, the HST Project System Engineering Board (HPSEB) found the detected level of variation significantly disturbing and consequently established a special working group to analyze, characterize, and, if possible, explain the changes. Significant support for the efforts of the FGS Working Group (FGSWG) was provided from many sources. Besides the current authors, the group consisted of, or received support from, HDOS optical analysts and engineers, members of the Space Telescope Astrometry Team (STAT), representatives of the HPSEB, and staff scientists at the Space Telescope Science Institute (STScI). The efforts of the working group over the past 2 years have resulted in substantial advances in our understanding of the functioning of the FGSs and our ability to maintain a precise level of calibration for them. We believe that this enhanced understanding will prove particularly important for the operation of the HST during the post-FSM era.

Each of the various subgroups within the FGSWG had its own area of particular concern. Not surprisingly, these areas overlapped to a considerable extent. The particular goal of the authors of this paper was to establish an FGS calibration program adequate to meet the operational needs of the HST mission as a whole. The calibration software used for this work is part of the HST Payload Operations Control Center (POCC) Applications Software Support (PASS) system developed by Computer Sciences Corporation (CSC); Ref. 3 documents the PASS system requirements. Analyses by the STAT were analogous to our own but focused on the use of the FGS system, and particularly FGS-3, as a tool for doing high-precision astrometric science. To distinguish our work from that of the STAT, we refer in this paper to the results of the two groups as the PASS and STAT solutions, respectively. HDOS analysts provided technical expertise for understanding the hardware, both of the FGSs and of the primary and secondary mirror structure of the telescope. The calibration analyses performed by

the PASS and STAT groups were done in friendly competition. The work was a competition in that the details of the algorithms and software were developed independently and thus could be used for mutual verification. The competition was friendly in that the verification and exchange of results were done on a regular basis. This approach provided valuable feedback for both groups, allowing early detection of analysis errors and a more timely arrival at our mutual goals.

2. THE FINE GUIDANCE SENSORS

The heart of the HST's pointing control system (PCS) is the set of FGSs manufactured specifically for use on the HST by HDOS. A description of FGS design and operation is available in Ref. 4, with indepth descriptions available in Ref. 5. We limit ourselves here to a high-level summary needed as a foundation for the results presented in the rest of the paper. The FGS FOVs are restricted to the outer 4-arcminute annulus of the HST's full FOV. Each FGS FOV is an arc with an azimuthal range of 82 degrees and a radial range extending from 10 arcminutes to 14 arcminutes relative to the primary optical axis of the telescope. Figure 1 illustrates the FOVs of the FGSs as they look out to the celestial sphere. The axis labels (V2,V3) indicate the HST coordinate frame; the third axis, referred to as V1, corresponds to the optical axis and points out to space. The visual magnitude (m_v) range for guide stars usable by the FGSs is approximately 9 to 14.5 m_v . The precision of the FGS system, ~ 3 mas when fully calibrated, follows from its design as an amplitude interferometer using

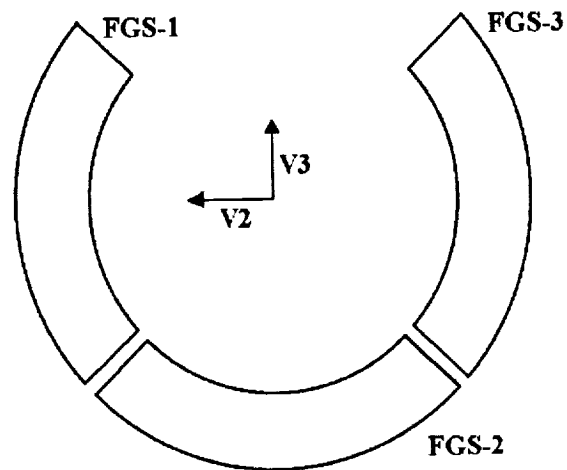


Figure 1. FGS fields of view (looking out to the celestial sphere)

Koester's prisms combined with photomultiplier tubes. Standard pointing control procedure during scientific observations is to use two of the FGSs to maintain guidance of the spacecraft. The remaining FGS is available for precise astrometric observations, the dim limit for astrometry being $\sim 17 m_v$.

Figure 2 illustrates the coordinate system of an FGS as it maps to the actual hardware and telemetry from the spacecraft. Each FGS coordinate frame is defined as a right-handed $x/y/z$ system with the z -axis pointed approximately along the HST optical axis. Each FGS has a 5-arcsecond-by-5-arcsecond instantaneous field of view (IFOV) that can be commanded to a selected position within the total FGS FOV. The instantaneous position of the center of the IFOV is determined by the angles θ_A and θ_B in Figure 2. The lengths of the "lever arms" δ_A and δ_B indicated in Figure 2 map onto specific aspects of the hardware design; for the purposes of this discussion the lever arms may be thought of as rigid, hinged rods whose rotations move the IFOV about in the total FOV. Using spherical trigonometry (e.g., see Ref. 6), the equations that transform the angles θ_A and θ_B into standard spherical polar coordinate angles ρ and ϕ can be derived:

$$\rho = \cos^{-1} [\cos(\delta_A) \cos(\delta_B) - \sin(\delta_A) \sin(\delta_B) \cos(\theta_B - (\theta_A - \theta_{A0}))] \quad (1)$$

$$\phi = (\theta_A - \theta_{A0}) + \cos^{-1} [(\cos(\delta_B) - \cos(\delta_A) \cos(\rho)) / (\sin(\delta_A) \sin(\rho))] \quad (2)$$

where θ_{A0} is an offset parameter to be determined via the calibration process. (An analogous offset parameter for θ_B is not required because any constant term added to both θ_A and θ_B is observationally indistinguishable from a rotation of the sensor; this can be absorbed in the subsequent alignment calibration.) The FGS can detect star light only through the IFOV. A star image falling within the inner 20 mas of the IFOV will produce a significant interferometric signal. The FGS is said to be in fine lock (FL) when so measuring a star's direction. Further spherical trigonometric manipulation is needed to adjust for the star's measured position relative to the center of the IFOV. Although included in our data analysis, these complications will not be considered here; rather the coordinates ρ and ϕ will be treated as if they were the coordinates of the measured star position in the FGS FOV. The equations that transform ρ and ϕ

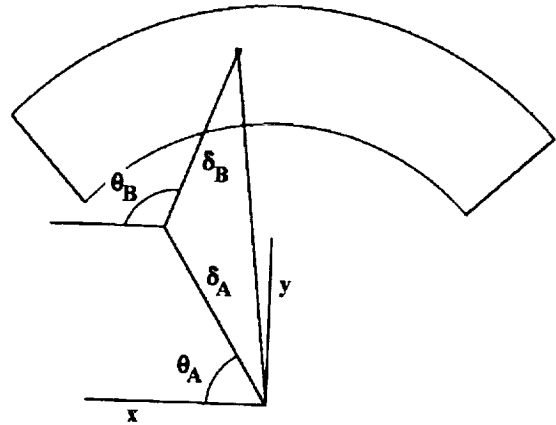


Figure 2. FGS coordinate system

into the x and y Cartesian elements of an object space unit vector are

$$x = \sin(\rho/M) \cos(\phi) \quad (3)$$

$$y = \sin(\rho/M) \sin(\phi) \quad (4)$$

where M , the magnification of the HST/FGS system, is approximately 57.3. We have found that M may be taken as fixed during calibration of the sensors, with scale adjustments being introduced via changes to the parameters δ_A and δ_B .

A second mode of FGS operation, coarse track (CT) mode, is also available. In this mode the center of the IFOV is commanded to nutate about the true star position in such a way that the edges of the IFOV cut across the image of the star in a symmetric pattern. The coordinates ρ and ϕ are then estimated as the center of the nutation circle. The estimated design accuracy of determining star positions using CT mode is approximately 20 mas. Because CT mode is less sensitive to spacecraft-jitter-induced loss of lock than is FL mode, it is sometimes used in observing situations for which extreme pointing precision is not required.

3. CALIBRATION ALGORITHMS

3.1 Distortion and Scale Determination

The distortion and scale calibration of the FGSs is divided into two phases. The first (also called "mini") phase uses ground-based astrometric observations as reference information and is thereby limited by the accuracy of those data. The second

(also called "full") phase goes beyond the limitations of ground-based astrometric work, the goal being to achieve the design precision of the FGS system. To date, full-OFAD calibration has been performed only for FGS-3, the FGS selected for use in astrometric science. A phase 1 scale calibration for an FGS follows immediately as part of a mini-OFAD calibration; the ground-based observations serve to define the absolute scale for the solution. Phase 2 scale determination, which is planned to be based on asteroid observations and associated precise theoretical ephemerides, has not been performed for any of the FGSs as of the time of this writing. Refs. 1 and 2 describe the algorithm and procedures intended for that calibration.

The algorithm used for OFAD calibration is a constrained two-dimensional least-squares algorithm based on the technique presented in Ref. 7. The fundamental input data are FGS observations of stars in an open cluster. The data are taken over a number of spacecraft pointings. Any given star may therefore be observed in multiple locations in the FGS FOV during the course of the entire sequence. Before being processed through the calibration algorithm, the data are corrected for the effects of velocity aberration using a fully relativistic formulation (e.g., see Ref. 8). The approach thereafter is to minimize a loss function, L , subject to certain constraints applied to the associated state vector. The loss function can be expressed as

$$L = \sum \{ [W_{ij} - D(W_{ij}, S) - A_j X_i]^2 / \sigma_{ij}^2 \} \quad (5)$$

where

- W_{ij} = object space position of star i in observation set j (as determined by equations 1 through 4)
- $D(W_{ij}, S)$ = OFAD correction vector function
- S = OFAD correction function parameter set
- A_j = attitude transformation matrix between attitude frame j and an arbitrarily specified standard frame
- X_i = "true" direction vector for star i in the standard frame
- σ_{ij} = measurement uncertainty for star i in set j

and the summation is done over all stars and frames. (The term "frame" here refers to data taken in a single orbit, during which a single pair of guide stars is used to control the vehicle's attitude.) For HST

OFAD calibration, the correction function $D(W_{ij}, S)$ has been parameterized as separate polynomials in the x and y Cartesian projections of W ; the set $\{S\}$ is the corresponding set of polynomial coefficients.

The state vector for a mini-OFAD calibration (which can in principle be done with a single spacecraft pointing and each star observed only once) consists of the set $\{S, A, \delta_A, \delta_B, \theta_{A0}\}$, i.e., the polynomial coefficients, attitude transformation matrices, and three star selector parameters. The vector set $\{X\}$ is provided as a priori knowledge from ground-based observations. It need be accurate only differentially; any systematic errors in $\{X\}$ will be absorbed in the matrices $\{A\}$. Three constraints must be applied because any average translation or rotation introduced into the function D via changes to $\{S\}$ would be indistinguishable from a systematic rotation of the spacecraft applied to all matrices $\{A\}$; without constraints, the associated matrix inversion problem would be singular (or nearly so) with a nullity of 3. To select a unique solution from an infinite potential family of solutions, we impose constraints on the elements $\{S\}$ such that the calculated change in D relative to an initial estimate has zero translation and rotation content when averaged across the FGS FOV.

The full-OFAD calibration procedure extends the mini-OFAD procedure so as to include the vector set $\{X\}$ as part of the state vector, thereby eliminating all errors associated with ground observations. Because the reference frame for $\{X\}$ is arbitrary, one of the attitude matrices is eliminated by selecting the associated observation frame as the standard frame. Unlike mini-OFAD calibration, full-OFAD requires multiple frames of data and significant variation of the spacecraft attitude between frames. In particular, the full-OFAD algorithm requires that there be significant variation in spacecraft roll to detect any shear effects in distortion. It is by moving the various target stars through locally different distortion variation in the FGS FOV that the relative distortion across the entire FOV becomes observable. Numerical simulations performed by the STAT have demonstrated that roughly 20 observation sets are required to achieve milliarcsecond accuracy for the function D . As with mini-OFAD computations, full-OFAD calibration requires that constraints be applied to the state vector. In addition to the three constraints discussed for the mini-OFAD algorithm, two constraints related to solution scale are used in the PASS software. Because the set $\{X\}$ is part of the

state vector of the problem, true scale is intrinsically nonobservable to the full-OFAD algorithm. To first order in the state vector elements, a change in the scale of $\{X\}$ (i.e., in the calculated angular distance between cluster members) can be compensated for by a change in the polynomial set $\{S\}$ and/or the star selector parameters $\{\delta_A, \delta_B\}$ with no increase in the loss function. To remove this second-order singularity from the full-OFAD problem, one constraint each is applied to the sets $\{S\}$ and $\{\delta_A, \delta_B\}$. The constraint on $\{S\}$ is applied in a manner analogous to those used to prevent $\{S\}$ from introducing changes in translation or rotation; it prevents D , when averaged across the FGS FOV, from changing its scale properties. The constraint applied to $\{\delta_A, \delta_B\}$ is simply that the sum $\delta_A + \delta_B$ remain unchanged. These constraints are adequate to allow the full-OFAD algorithm to pick out a unique solution.

Although the algorithm described in the previous paragraph is able to select a solution that is both unique and a minimum of the full-OFAD loss function, the scale content for the solution so produced is only approximately correct. This occurs primarily because the unconstrained parameter θ_{A0} is capable of introducing both scale and distortion contributions to the solution. Given that, to date, astrometric ground-based catalogs represent the best source of true scale information for the target clusters that we have been using, we have chosen to rescale our full-OFAD solution using the mini-OFAD algorithm. The data are reprocessed with the state vector restricted to the set $\{A, \delta_A, \delta_B\}$ subject to the constraint that the ratio δ_A/δ_B remain unchanged. With the set $\{\{S\}, (\delta_A/\delta_B)\}$ fixed to that found by the full-OFAD solution, and the rescaling introduced via the change to $\delta_A + \delta_B$ kept small, we find that this rescaling procedure introduces a negligible change to the distortion aspect of the solution. Finally, to produce a rescaled catalog of star positions based on the FGS observations, we rerun the full-OFAD algorithm using the restricted set $\{A, X\}$ as the state vector.

3.2 Alignment Determination

To date, the relative alignment of the FGSs has been determined only with an accuracy commensurate with astrometric ground-based observations. Before HST launch, plans had been made to eventually perform this alignment calibration to the full design accuracy of the sensors; Refs. 1 and 2 discuss the

algorithm intended for this purpose. As a consequence of the fairly rapid temporal variations that we have found in the relative alignments of the FGSs, it has been decided that the effort that would be required to achieve full FGS accuracy is unwarranted. Rather, procedures and software have been developed that permit monitoring of the changes in the alignments as a function of time. The approach begins with an alignment determination that uses ground-based observations of target stars as fiducial points. With the relative alignments specified, observations from all three FGSs can be used to construct a catalog against which future observations of the same stars can be compared. Apparent changes in angular separation between stars observed in different FGSs during repeat visits to the target cluster are then used to determine relative alignment shifts between the FGSs.

As described in Refs. 1 and 2, there exists a systematic offset for each FGS between a star's position as determined using CT mode and that found using FL mode. These offsets must be accounted for during relative alignment determination if any of the data were taken with one or more of the FGSs operating in CT mode. HST operating conditions were sufficiently degraded during the first year of operations as to mandate the use of CT guidance during FGS calibration data takes. Our fiducial data set for relative FGS alignment determination was taken during this time period and was corrected for the CT/FL offset effect with data obtained concurrently. Because the 20-mas accuracy level of coarse track guidance is comparable to the best ground-based astrometric catalogs, degradation of alignment results as a consequence of using CT guidance is not severe.

4. REFERENCE CATALOGS

Two target clusters have been used for FGS calibration work to date: the open clusters NGC 5617 (r.a. $\sim 217^\circ$, dec. $\sim -60^\circ$) and M35 (r.a. $\sim 93^\circ$, dec. $\sim 24^\circ$). An NGC 5617 astrometric quality reference catalog based upon ground observations was provided for mini-OFAD and alignment calculations by the astrometry group at Yale University (Ref. 9). An analogous catalog for M35, based upon the observations of McNamara and Sekiguchi (MS, Ref. 10), was provided to us by the STAT. The estimated 1σ random error levels associated with the Yale and MS catalogs are 30 and 24 mas, respectively, based upon an intercomparison of results from separate plates. Both catalogs

contain proper motion estimates for the included stars. We used these estimates to correct for the effects of proper motion when comparing any sets of data taken on different dates.

One result of the FGS OFAD analysis over the past few years is the discovery that the position coordinates for the stars in both ground catalogs were subject to significant magnitude and color dependencies relative to the FGS data. The levels of these systematic dependencies were such that the standard deviations of residuals to mini-OFAD fits were 70 and 41 mas for NGC 5617 and M35 data, respectively. Because FGS data are intrinsically more accurate than ground observations, the scatter of mini-OFAD residuals should be essentially the same as the estimated intrinsic catalog error level; larger mini-OFAD residuals are an indication of systematic catalog error. This effect was first recognized for the Yale catalog a few months after associated FGS observations were made in December 1990. The Yale group subsequently corrected its catalog, using the results of a preliminary FGS full-OFAD calibration as a basis for the correction. The resulting standard deviation for mini-OFAD residuals was reduced to 35 mas, in reasonable agreement with the estimated intrinsic random catalog error. The corrected Yale catalog was used in the analysis reported in this paper.

As a consequence of the discovery of the magnitude and color dependencies in the original Yale catalog, the PASS system was augmented to include software to compare star catalogs for relative magnitude and position dependencies. The use of this utility became a planned feature in the cycle of mini-OFAD and full-OFAD calibration processing. The first step is to produce preliminary mini-OFAD and full-OFAD solutions based upon a completely independent ground catalog. The catalog produced as part of the full-OFAD solution is then used as a reference against which the ground catalog may be compared for determining magnitude and color dependencies. Corrections for any so-detected dependencies may then be removed from the ground catalog, after which the cycle of mini-OFAD and full-OFAD processing is repeated. This procedure was applied during our analysis of observations of M35, with the result that the standard deviation for associated mini-OFAD residuals was reduced to 22 mas, in good agreement with the 24-mas estimate from interplate comparisons. This corrected version of the MS catalog was used in our subsequent analysis.

The reader may reasonably ask how it is known that the errors to be corrected are within the ground data as opposed to the FGS data. As a first point, when performing a mini-OFAD calibration with multiple frames of data, we find that the postfit observation residuals are strongly correlated in both size and direction in sky coordinates for all observations of any individual star; this indicates that the error source is associated with the individual stars and not with FGS FOV position. Second, with respect to NGC 5617 data, the same correction relative to sky coordinates was found for all three FGSs. Given that the FGSs had different relative orientations on the sky during the observations (see Figure 1), it is unlikely that the FGSs themselves could produce such an effect. Finally, with respect to M35 data, a single correction relative to sky coordinates is found to be appropriate irrespective of spacecraft roll. This eliminates both the FGS used for these observations (FGS-3) and the HST primary and secondary mirror system as possible sources of the magnitude/color effects. For these reasons, we find it appropriate to attribute the effects to the ground catalogs.

5. CALIBRATION RESULTS

5.1 Distortion and Scale Results

5.1.1 Previous Results

Several unanticipated operational constraints significantly affected the ability of HST in general, and the FGSs in particular, to acquire FGS calibration data during the first years of HST operations. Of these, the most serious from our perspective was the spacecraft jitter induced at day-night transitions by the thermal flexing of the original solar arrays. Jitter-induced loss-of-lock for FGS guide stars remained a serious problem until a guide star recentering algorithm was implemented in the flight software in December 1992. As a consequence, all FGS calibration data were taken using CT guidance during the first 2 years of the mission. During this period, peak-to-peak spacecraft pointing changes as high as 100 mas were noted, although at a sufficiently high frequency that averaging across the 1-minute observation periods for each astrometry star significantly reduced the pointing error. Maximum average displacements of the guide stars during a single orbit were typically on the order of 10 mas. Using this level of performance, the first reasonably successful mini-OFAD calibration was completed in December 1990.

In Refs. 1 and 2, we discussed calibration results for data taken in December 1990 and May 1991, reporting that the measured values for the distortion coefficients agree reasonably well with their design values for all three FGSs, but the parameter θ_{A0} differs significantly from its design value of zero for both FGS-2 and FGS-3. θ_{A0} is approximately 0.57° and -0.63° for FGS-2 and FGS-3, respectively. Prelaunch analysis indicated that ground-to-orbit changes in θ_{A0} would be less than 0.1° . The cause of these large deviations remains unexplained. A comparison of the OFAD results between December 1990 and May 1991 indicated that significant changes had apparently occurred during the 5-month interval. Given the restricted accuracy of the data sets, it was possible then to characterize the change only to first order — and only as an approximate scale change. The largest change was detected for FGS-1, for which the effective scale change corresponded to 100 mas over 14 arcminutes. The estimated accuracy of the December 1990 and May 1991 mini-OFAD calibrations is about 10 mas over FOV regions separated by no more than about 4 arcminutes and about 30 mas across the whole FOV of any single FGS.

5.1.2 New Results

Since the writing of Refs. 1 and 2, three major advances in our analysis of FGS distortion have occurred. First, via differential studies of apparent changes in star positions during repeat visits to the calibration target clusters, we have been able to better quantify the nature of the long-term "scale" variations previously reported. Second, via repeat observations of selected "check" stars during periods of continuous astrometric observing, we have found significant apparent changes in the effective relative alignments of the FGSs over time periods short compared with a single orbit. Finally, because of the operational improvements in fine lock guiding performance made possible by flight software enhancements, a full-OFAD calibration observing sequence for FGS-3 became possible and was successfully executed in January 1993. The advances in our understanding of FGS performance occurred over a period of months, with improvements in each area providing a better foundation for analysis in the others. Although we discuss each area separately below, their interdependence is readily apparent.

5.1.2.1 Long-Term Variations in Distortion

Our studies of the long-term variations of the FGS distortion calibration are based on two sequences of

OFAD data sets. The first provided us with a 2-year baseline starting with our original December 1990 mini-OFAD calibration observations of the star cluster NGC 5617. As previously noted, the accuracy of this initial calibration is estimated to be about 10 mas over small regions of each FGS FOV and about 30 mas over each complete FOV. To take advantage of the relatively good calibration accuracy over small FOV regions, we based our analysis of calibration changes on differential studies of apparent changes in star positions during repeat visits at 1-year intervals to the same target cluster. The 1-year interval was dictated by spacecraft operational pointing constraints; spacecraft roll relative to the sunline is constrained to prevent illumination of the underside of the spacecraft. By repeating the observations at 1-year intervals, we were able to place the various target stars in essentially the same position in the FOV as during the initial calibration. After compensating for proper motion effects, we determined the adjustments to our December 1990 solution needed to restore the original relative positions. We found, to within the accuracy of our data, that the FGS calibration changes are well modeled as changes to the star selector parameters δ_A and θ_{A0} . Although adjustment to both parameters is in general required for good modeling at the data noise level, we find that the FGS-1 variation is greatly dominated by changes to θ_{A0} ($\Delta\theta_{A0} \cong -0.044^\circ$ over 2 years), whereas that for FGS-3 is greatly dominated by changes to δ_A ($\Delta\delta_A/\delta_A \cong 2.9 \cdot 10^{-4}$ over 2 years). The 2-year variation over baselines of about 12 arcminutes was roughly 200, 30, and 100 mas for FGSs 1, 2, and 3, respectively.

Because of the long-term changes in distortion calibration observed for all three FGSs, it was decided that a high-accuracy monitoring program should be established for FGS-3, the FGS selected for astrometry work, as a companion activity to its full-OFAD calibration. This long-term stability (LTSTAB) program began 1 month before the January 1993 full-OFAD observing sequence. M35 is the selected target for both the full-OFAD and the LTSTAB calibration work. Because M35 is located near the ecliptic plane, spacecraft roll constraints dictate two possible principal roll orientations of the spacecraft relative to the target. Using data from any specific orientation, it is possible to conduct purely differential studies of FGS distortion changes; such studies are not subject to errors in a specific OFAD solution or a selected reference catalog. With only slightly greater error, a

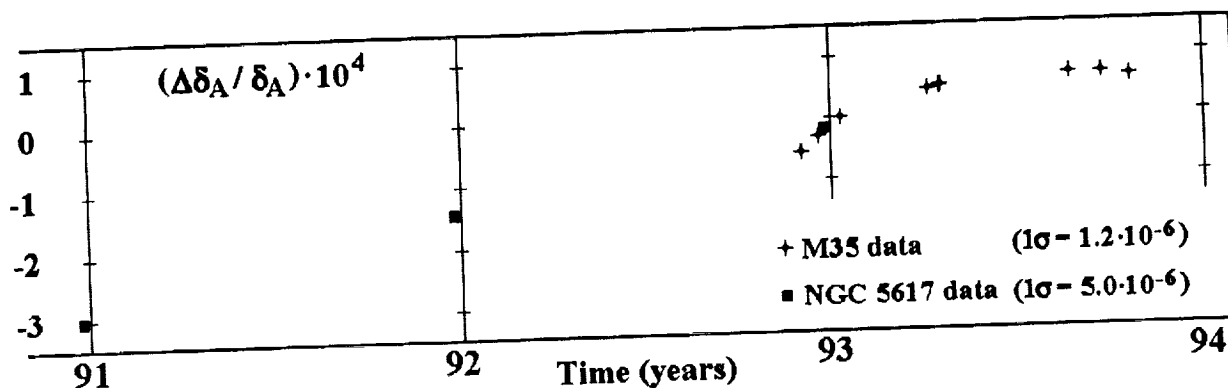


Figure 3. For FGS-3, long-term variation of parameter δ_A as a function of time

combined LTSTAB study can be performed using data from both orientations by taking advantage of the results from a full-OFAD calibration; the OFAD solution is used to correct for distortion, and the FGS-generated catalog serves as an orientation independent set of reference points. We have selected the latter approach for the results presented here, using our analysis of the January 1993 full-OFAD data set as our fundamental reference.

As was the case for the NGC 5617 observations, most of the temporal changes in FGS-3 distortion are fairly well modeled by adjustments to the single parameter δ_A . Figure 3 presents a plot of the change in δ_A as a function of time, with δ_A treated as the only free distortion parameter. The plot combines the results of the differential studies using observations of stars from both NGC 5617 and M35. Relative normalization of the two data sets was accomplished by placing the NGC 5617 December 1992 data point on a smoothly interpolated position within the M35 sequence. (The normalization is consistent with the scale of both ground catalogs to within their error levels.) The results suggest that the variation of δ_A is significantly nonlinear for time scales between a few months and 1 year but fairly linear for time scales of order 2 to 3 years. LTSTAB monitoring of FGS-3 distortion will continue for the indefinite future, with the results being used for both engineering analysis of FGS performance and correction of astrometry data obtained with that sensor.

5.1.2.2 Short-Term Alignment Variations

The second area of analysis advancement pertains to the apparent change in relative FGS alignments over time periods comparable to a single orbit. For all of our recent OFAD calibration data sets, and in particular for the full-OFAD data obtained in

January 1993, the astrometry observing sequence includes repeat observations of three well-separated stars during the course of each orbit. The function of these "check" star observations is to detect any systematic change in the astrometry FGS FOV with respect to translation, rotation, or scale during the course of a single orbit. With a perfectly operating optical system, after compensation for velocity aberration effects, all of the check stars would maintain their angular separations relative to each other and to the guide stars monitored by the other two FGSs. (With an ideal pointing control system, the star positions — not merely their angular separations — would also remain fixed.) In practice, the angular separations do not behave as they should for a perfect system; significant systematic motion of the check stars relative to the two "fixed" guide stars is regularly seen to occur. The effective change in alignment during a typical 40-minute observing sequence is on the order of 10 mas, although one orbit showed a change as large as 17 mas. Changes in the effective alignment of the astrometry FGS relative to the guiding FGSs over a single observing period result in a motion of the astrometry FOV relative to the background stars. If left uncorrected, this effect would corrupt the OFAD calibration.

Investigation of the phenomenon of short-term FOV motion has been undertaken from two perspectives: (1) to model and remove the effect from FGS calibration data (or astrometry science data, for that matter) and (2) to understand the physical cause of the phenomenon. Clearly the latter objective can be an important intermediate goal on the way to the former, but achieving complete success in that area is not necessary to make significant first-order corrections to the data. We have found that the check star motion for FGS-3 astrometry orbits is fairly well modeled as constant velocity translation

of the whole FOV, the model being extremely good for about two-thirds of such orbits. We have therefore used this model in conjunction with check star data to establish FOV-motion parameters for each orbit of our full-OFAD and LTSTAB data sets and thereafter applied the model to correct all of the remaining astrometry observations within each orbit.

The cause of this apparent motion of the astrometry FOV relative to the FOVs of the guide FGSs is not yet well understood. A conjecture was made a couple of years ago that differential heating of the secondary mirror support structures could cause the mirror to move and produce focus and coma changes that would result in the observed behavior. Christ Ftaclas at HDOS has developed an optical model for the implied effects for FGS observations and found it to work well for about half of the January 1993 OFAD calibration orbits. The motions in the remaining orbits are incompatible with the model, being either wrong in direction or containing sharp changes. This may indicate the existence of yet another mechanism. A PCS/FGS coupling study has been initiated recently and may shed some light on this phenomenon. Evidence for secondary mirror "breathing" has also been seen in the data from the other HST scientific instruments (SIs). Investigating the conjecture that there is a thermal driver for the effect, Pierre Bely of the STScI has shown that there is a correlation between the temperature of HST's forward light shield and the changes observed by some SIs (Ref. 12). He further computed the changes to secondary mirror position needed to model these changes. Unfortunately, the amount of secondary mirror motion needed to model the changes in SI response is only about half of that needed in the Ftaclas model to explain concurrent apparent motions of the FGS FOVs. This difference is being investigated. If no significant error is found in either analysis, that may be taken as an indication for the existence of some mechanism that has an effect on the FGSs but not on the SIs. Again, the PCS/FGS coupling study may resolve this question.

Within the context of the Ftaclas model for FGS pointing changes, we find that the simplicity of our linear-motion correction procedure for FGS-3 astrometry data is somewhat fortuitous. The model predicts that effective rotation and scale changes also occur in the astrometry FGS FOV, but these effects happen to be below noise level for cases when FGSs 1 and 2 are used for guiding.

5.1.2.3 Full-OFAD Calibration

With the phenomenon of short-term alignment variation reasonably well modeled, and with the problem of jitter-induced loss-of-lock solved, a full-OFAD calibration at the level of FGS design accuracy became possible. For reasons of economy (i.e., because the amount of data required for the full calibration of a single FGS is large), it was decided to perform the calibration only for that FGS selected for use in astrometric science. Twenty frames of M35 observations for this calibration were acquired on January 10 and 11, 1993. Analysis was restricted to data obtained with all three FGSs in FL mode. Each star vector was constructed as an average over approximately 25 seconds of data. The observing period for each frame was roughly 35 minutes. Data from 2 of the 20 orbits were removed from consideration because of commanding and guidance problems.

We processed the data for distortion calibration using the algorithms discussed in Section 3. We began with an FGS-3 mini-OFAD solution based on data from the December 1990 and December 1992 observations of NGC 5617. The distortion portion of the state vector for this solution was restricted to the parameters $(\delta_A, \delta_B, \theta_{A0})$, the polynomial coefficients being held at their design values. Values for the three star selector parameters were first determined using the 1990 data; adjustments to (δ_A, θ_{A0}) were then determined based upon a differential comparison of the 1990 and 1992 data. The star selector parameters alone were adequate to define deviations from design distortion to roughly the accuracy of the ground catalog (~ 30 mas, 1σ), whereas adjustments to (δ_A, θ_{A0}) captured the 2-year differential changes to within the accuracy of the 1990 FGS data (~ 8 mas, 1σ).

Using the NGC 5617 mini-OFAD solution as an initial estimate, we processed the M35 data through the full-OFAD algorithm to generate an intermediate solution star catalog with which to correct the MS catalog (Ref. 10). The state vector for this solution consisted of coordinates for the 91 observed stars, 3 star selector parameters, 14 polynomial distortion coefficients (up to third order), and attitude Euler angles. The single-axis standard deviation of residuals for the fit was 3.3 mas. As described in Section 4, we used the FGS-generated star coordinates catalog to correct the MS catalog. (The correction was dominated by the dependency on magnitude, the size being 36 ± 6 mas / m_V .) The

corrected MS catalog and the 18 frames of FGS M35 data were then used in a mini-OFAD calculation. The state vector for this solution consisted of the star selector parameters, 15 distortion polynomial coefficients, and attitude Euler angles. As described in Section 3, three constraints were applied to the distortion polynomial to prevent any meaningless change in translation or rotation content. The single-axis standard deviation for the postfit residuals of this solution was 22 mas.

The state vector for the subsequent full-OFAD calculation consisted of the 3 star selector parameters, 21 polynomial coefficients, 51 Euler angles, and coordinates for the 91 stars. Five constraints were applied: the four translation, rotation, and scale polynomial constraints and the single ($\delta_A + \delta_B$) constraint. The single-axis standard deviation of residuals for this fit was 2.5 mas. (After adjustment for the dimension of the state vector, this translates into an estimate for the intrinsic root-mean-square FGS measurement error of 2.8 mas.) As discussed in Section 3, rescaling of this OFAD solution using the mini-OFAD algorithm was required because changes in θ_{A0} generate scale changes as well as distortion changes. Based on the accuracy of the MS catalog and the number of stars observed, we estimate the scale accuracy of our final OFAD solution to be good to 1 part in $2.5 \cdot 10^5$ (roughly 3 mas over a 12-arcminute arc). A final FGS-based M35 catalog was then generated using the full-OFAD software with the state vector restricted to the attitude Euler angles and the relative star coordinates. The 2.5-mas standard deviation of residuals was preserved through this rescaling process, verifying the basic validity of the approach.

Our final results agree well with the independent calibration work performed by the STAT (Ref. 13), which found a solution characterized by a standard deviation of the residuals of 2.3 mas. The slightly tighter residuals found in the STAT solution are probably a consequence of the team's incorporation into their algorithm of a spacecraft jitter correction based upon observations of the guide stars at time points coincident with the astrometry observations. The two-axis root-sum-square error in a single observation implied by the calibration results is 3.5 and 3.2 mas for the PASS and STAT solutions, respectively, which agrees well with the prelaunch expectation of 2.7 mas.

5.2 Alignment Results

Refs. 1 and 2 presented our early relative alignment determination results for the three FGS FOVs. The first determination was based on 17 frames of NGC 5617 data taken in December 1990. Each frame contained observations of 2 guide stars and about 10 astrometry stars, FGS-2 being used for astrometry. Corrections for velocity aberration, distortion, scale, and CT/FL offset were applied before determination of the relative FOV alignments. The Yale catalog was used to provide the fundamental reference set of angular separations. The postcalibration standard deviation of residuals for the difference between measured and reference star separations was found to be 35 mas, consistent with the estimated accuracy of the reference catalog. Subsequent observations in January 1991 and May 1991 indicated apparent relative shifts of the FGS FOVs. The alignment change was manifest primarily as motions in opposite directions parallel to the V3-axis by the FGS-1 and FGS-3 FOVs relative to FGS-2, the magnitude of the shifts being of order 200 mas after 5 months.

The repeat visits to NGC 5617 in December 1991 and December 1992 have allowed a continued monitoring of the long-term changes in the relative alignments of the FGSs. Specification of the changes in the relative alignments of the FGSs is coupled to the assumed form of any changes to the individual responses of the FGSs. Different effective alignment shifts are seen depending on the model used to represent distortion changes. Our decision to represent distortion changes using the parameters δ_A and θ_{A0} influences our alignment change results significantly, but ultimately only at a level of order 10 percent of the detected alignment change. Our differential method for determining the relative alignment changes from December 1990 to December 1991 and December 1992 is discussed in Section 3. The December 1991 data were acquired in a repeat of 4 of the previous year's alignment determination orbits; the December 1992 data were acquired in a repeat of 3 of the December 1990 OFAD determination orbits, with each FGS in astrometry mode once. The December 1991 ($\Delta V2$, $\Delta V3$) shifts in effective coordinate grids for FGS-1 and FGS-3 relative to FGS-2 were (110, -160) mas and (370, 690) mas for FGS-1 and FGS-3, respectively; the December 1992 shifts were (120, -660) mas and (530, 1030) mas for FGS-1 and FGS-3, respectively. Roll changes were small and have not been included here. The standard deviation for the residuals in

these differential fits was about 10 mas. The relative shear between FGS-1 and FGS-3 increased from about 850 mas in December 1991 to nearly 1700 mas in December 1992.

The physical cause of this continued change in the relative alignments of the FGSs remains under investigation. Some significant progress has been made by HDOS optical engineers via a study of data taken using the internal test source (ITS) for each FGS. Ideally, the coordinates of each ITS should remain fixed with time. HDOS has found that the ITS coordinates are changing and that appropriate differences between the coordinate changes for FGSs 1 and 2 and for FGSs 3 and 2 are strongly correlated with the changes reported for the relative alignments of the FGS FOVs. (Three of the four comparable coordinate differences agree to within about 20 percent for the two different procedures.) This suggests that the effective alignment changes are occurring as a result of changes internal to the individual FGSs. As part of its general effort to characterize the on-orbit changes in the HST/FGS system (Ref. 14), HDOS conducted an optical sensitivity study that indicated that motion of the FGS asphere could cause relative alignment changes of the detected size. The physical mechanism that drives the motions remains unclear.

6. SUMMARY

This paper has presented a review of the procedures and algorithms used for the calibration of the HST FGSs, as well as a discussion of the results obtained through the end of 1993. Despite the well-publicized problems with HST discovered shortly after launch in April 1990, significant progress has been made in calibrating the system to achieve good pointing performance. Design-level (~ 3 mas) distortion calibration for FGS-3 was achieved with data taken in January 1993. Distortion calibration at the 30-mas level has been achieved for the remaining two FGSs. Long-term trends in distortion variation have been measured and characterized for all three FGSs, and a long-term stability monitoring program has been put in place for FGS-3. Short-term (intraorbit) variations in the effective alignments of the FGS FOVs have been observed and adjusted for in the distortion calibration for FGS-3. Relative alignment calibration for the FGSs has been achieved at the 30-mas level. Systematic long-term changes in the relative FGS FOV alignments with rates on the order of 0.5 arcsecond per year have been found. Continued monitoring of,

and adjustment for, these changes in FGS distortion and alignment calibration will be an important feature of routine HST engineering calibration maintenance as HST scientists strive for full design performance from the telescope during the post-FSM era.

A great many individuals and organizations have been involved in the efforts that ultimately resulted in the successful calibration of the HST FGSs. Besides those already alluded to in the body of this paper, we would like to explicitly acknowledge the efforts of two individuals. Paul Davenport (GSFC/CSC) served as lead system engineer for the HST operations management system through the years of its development before launch; his analytic insights provided the basis for, or extensions of, many of the algorithms in the PASS system. Keith Kalinowski (GSFC) served as the chief representative of the HST project office to the FGSWG. His dedicated efforts and technical insights were invaluable to all aspects of the FGSWG investigations, but particularly with respect to the selection and preparation of the M35 observing scenarios used for the OFAD calibration.

The work reported in this article was supported in part by NASA contracts NAS 5-31500 (Welter), HB80E4940N (Abramowicz-Reed), NAS 5-31786 (Guha), and NAS 5-31000 (Kimmer), which enable CSC, HDOS, AKG, and ATSC to provide systems engineering, analysis, and operations support to NASA/GSFC.

7. REFERENCES

1. G. Welter, *The In-Flight Calibration of the Hubble Space Telescope Attitude Sensors, Proceedings of the GSFC Flight Mechanics / Estimation Theory Symposium - 1991*, NASA Conference Publication 3123, May 1991.
2. G. Welter, L. Abramowicz-Reed, A. Guha, L. Hallock, and E. Kimmer, *The In-Flight Calibration of the Hubble Space Telescope Fine Guidance Sensors, Proceedings of the Third International Symposium on Spacecraft Flight Dynamics*, ESA Publication SP-326, October 1991.
3. L. Hallock et al., *Space Telescope POCC Applications Software Support (PASS) Requirements Specification (Revision E)*, Computer Sciences Corporation Document CSC/TM-82/6045, September 1987.

4. A. Bradley, L. Abramowicz-Reed, D. Story, G. Benedict, and W. Jefferys, *The Flight Hardware and Ground System for Hubble Space Telescope Astrometry*, Publications of the Astronomical Society of the Pacific, March 1991, vol. 103, p. 317.
5. OAO Corporation, Hubble Space Telescope Astrometry Operations Handbook, Marshall Space Flight Center Document SMO-1040, March 1987.
6. W. Smart, Text-Book on Spherical Astronomy, Cambridge, England: Cambridge University Press, 1971.
7. W. Jefferys, *On the Method of Least Squares*, The Astronomical Journal, February 1980, vol. 85, no. 2, p. 177.
8. C. Misner, K. Thorne, and J. Wheeler, Gravitation, San Francisco: W. H. Freeman & Co., 1973.
9. T. Girard, C. Heisler, Y.-W. Lee, C. Lopez, W. van Altena, and P. Ianna, *Astrometric Calibration Regions with Proper Motion Membership Estimates in the Open Clusters NGC 188 and NGC 5617*, Poster Presentation at the January 1990 Meeting of the American Astronomical Society held in Washington D.C.
10. B. McNamara and K. Sekiguchi, *A Proper Motion Analysis of the Cluster M35*, The Astronomical Journal, March 1986, vol. 91, no. 3, p. 557.
11. C. Ftacclas and L. Abramowicz-Reed, *OFAD, Breathing, and the Shift Model*, Hughes Danbury Optical Systems Memorandum ST-SE-7160, April 6, 1993.
12. P. Bely, *Progress Report on Focus Change Study ('Breathing')*, Space Telescope Science Institute Technical Memorandum, December 4, 1992.
13. W. Jefferys, A. Whipple, Q. Wang, B. McArthur, G. F. Benedict, E. Nelan, D. Story, and L. Abramowicz-Reed, *Optical Field Angle Distortion Calibration of FGS3*, Proceedings of the HST Calibration Workshop, Space Telescope Science Institute, November 1993.
14. L. Abramowicz-Reed, R. Basedow, R. Crout, W. Freeman, C. Ftacclas, J. Tausanovich, and R. Zarba, Hubble Space Telescope Assembly Project - FGS Working Group Tiger Team Final Report, Hughes Danbury Optical Systems Report PR J14-0105, June 1992.

ACRONYM LIST

CSC	Computer Sciences Corporation
CT	coarse track
FGS	fine guidance sensor
FGSWG	FGS Working Group
FL	fine lock
FOV	field of view
FSM	First Servicing Mission
GSFC	Goddard Space Flight Center
HDOS	Hughes Danbury Optical Systems
HPSEB	HST Project System Engineering Board
HST	Hubble Space Telescope
IFOV	instantaneous field of view
ITS	internal test source
LTSTAB	long-term stability
M	Messier (catalog entry, e.g., M35)
mas	milliarcsecond
MS	McNamara and Sekiguchi (Ref. 10)
m_v	visual magnitude
NGC	New General Catalog (e.g., NGC 5617)
OFAD	optical field angle distortion
PASS	POCC Applications Software Support
PCS	pointing control system
POCC	Payload Operations Control Center
SI	scientific instrument
STAT	Space Telescope Astrometry Team
STScI	Space Telescope Science Institute

G. Welter, CSC, 1100 West Street, Laurel MD 20707

L. Abramowicz-Reed, HDOS, 100 Wooster Heights Road, Danbury CT 06810

A. Guha, AKG Inc., Post Office Box 10135, Silver Spring MD 20914

L. Hallock, Code 512.0, Goddard Space Flight Center, Greenbelt MD 20771

E. Kimmer, ATSC, Code 519.1, Goddard Space Flight Center, Greenbelt MD 20771